Quaternary Research 80 (2013) 88–98

Contents lists available at SciVerse ScienceDirect

Quaternary Research

journal homepage: www.elsevier.com/locate/yqres

A chronology for glacial Lake Agassiz shorelines along Upham's namesake transect

Kenneth Lepper [a,*], Alex W. Buell [a], Timothy G. Fisher [b], Thomas V. Lowell [c]

[a] Department of Geosciences, North Dakota State University, P.O. Box 6050/Dept. 2745, Fargo, ND 58108-6050, USA
[b] Department of Environmental Sciences, MS604, University of Toledo, Toledo, OH 43606, USA
[c] Department of Geology, 500 Geology/Physics Building, University of Cincinnati, Cincinnati, OH 45221-0013, USA

ARTICLE INFO

Article history:
Received 2 August 2012
Available online 6 May 2013

Keywords:
Lake Agassiz
Glacial lake
Strandlines
Optically stimulated luminescence dating
OSL

ABSTRACT

Four traditionally recognized strandline complexes in the southern basin of glacial Lake Agassiz are the Herman, Norcross, Tintah and Campbell, whose names correspond to towns in west-central Minnesota that lie on a linear transect defined by the Great Northern railroad grade; the active corridor for commerce at the time when Warren Upham was mapping and naming the shorelines of Lake Agassiz (ca.1880–1895). Because shorelines represent static water planes, their extension around the lake margin establishes time-synchronous lake levels. Transitions between shoreline positions represent significant water-level fluctuations. However, geologic ages have never been obtained from sites near the namesake towns in the vicinity of the southern outlet. Here we report the first geologic ages for Lake Agassiz shorelines obtained at field sites along the namesake transect, and evaluate the emerging chronology in light of other paleoclimate records. Our current work from 11 sampling sites has yielded 16 independent ages. These results combined with a growing OSL age data set for Lake Agassiz's southern basin provide robust age constraints for the Herman, Norcross and Campbell strandlines with averages and standard deviations of 14.1 ± 0.3 ka, 13.6 ± 0.2 ka, and 10.5 ± 0.3 ka, respectively.

Introduction

As early as 1823 the broad valley of the Red River of the North (Fig. 1) was recognized as a vast lake plain by W.H. Keating (Elson, 1983). G.K. Warren published an assessment of the boundaries of the lake in 1878 (Elson, 1983). But the lake, that continues to challenge us as Quaternary scientists, geomorphologists and geochronologists, was not named until 1890 by W. Upham (Elson, 1983). Warren Upham, in the employ of the Minnesota Geological Survey, the Geologic Survey of Canada, and the United States Geological Survey, conducted 15 yr of mapping and study of glacial Lake Agassiz resulting in his seminal 1895 monograph (Upham, 1895). This monograph includes extensive mapping of the lake's shorelines. In the southern basin these were grouped into 4 complexes. The names were assigned based on town sites in west-central Minnesota where the Great Northern Railroad line crossed shorelines. From south to north the towns and strandline complex names are: Herman, Norcross, Tintah, and Campbell. A fifth shoreline complex, the Upham, between the Norcross and the Tintah, has also been mapped. This strandline was proposed by Fisher (2005) because he found in the southern basin many strandlines including spits at an elevation of 311–314 m (1020–1030 ft) between the Norcross and Tintah levels. Ages for the Upham level may be found in Lepper et al. (2007) and are discussed in a later section.

With the advent of global positioning systems, space platform-based SRTM digital elevation models (DEMs), and most recently LiDAR DEMs, strandlines are more clearly resolved for analysis. Mapping by Brevik (1999) in North Dakota recognized the importance of using detailed soil maps in conjunction with geomorphology. Rayburn (1997) tracked the Upper and Lower Campbell north of 49°N using GPS units resulting in a new isobase map (Rayburn and Teller, 2007). Using SRTM DEMs and topographic maps, strandlines in the southern basin were quantified by a histogram analysis (Fisher, 2005) and the slopes of strandlines increasing to the north have been calculated initially by Upham (1895) and Johnston (1946), and more recently by Weller and Fisher (2009) and Yang and Teller (2012). As chronometric dating methods were not available to Upham, he interpreted the strandlines to represent sequential lowering of lake levels in the basin from the Herman to Campbell level (Upham, 1895).

The effort to assign ages for the evolution of Lake Agassiz goes back several decades. The first modern synthesis (Elson, 1967) suggested initial high levels that, with several oscillations, gradually fell over several thousand years. Details of this basic pattern have changed as new data have become available and as radiocarbon dating has improved. However, many of the stratigraphic controls presented in Elson (1967) bracket, rather than define, various water planes. Other ages incorporated in Elson's (1967) synthesis have been questioned because of the dating techniques used, material employed, or stratigraphic relationships (cf. Fisher and Lowell, 2006). See also the supplemental materials for a review of the first radiocarbon dates and lake-level history. It therefore remains a challenge to generate direct chronological control for the Lake Agassiz water levels.

Perhaps the best dated water level by radiocarbon techniques is the Campbell strandline. One key site is Wampum (Risberg et al.,

* Corresponding author. Fax: +1 701 231 7411.
E-mail address: ken.lepper@ndsu.edu (K. Lepper).

0033-5894/$ – see front matter © 2013 University of Washington. Published by Elsevier Inc. All rights reserved.
http://dx.doi.org/10.1016/j.yqres.2013.02.002

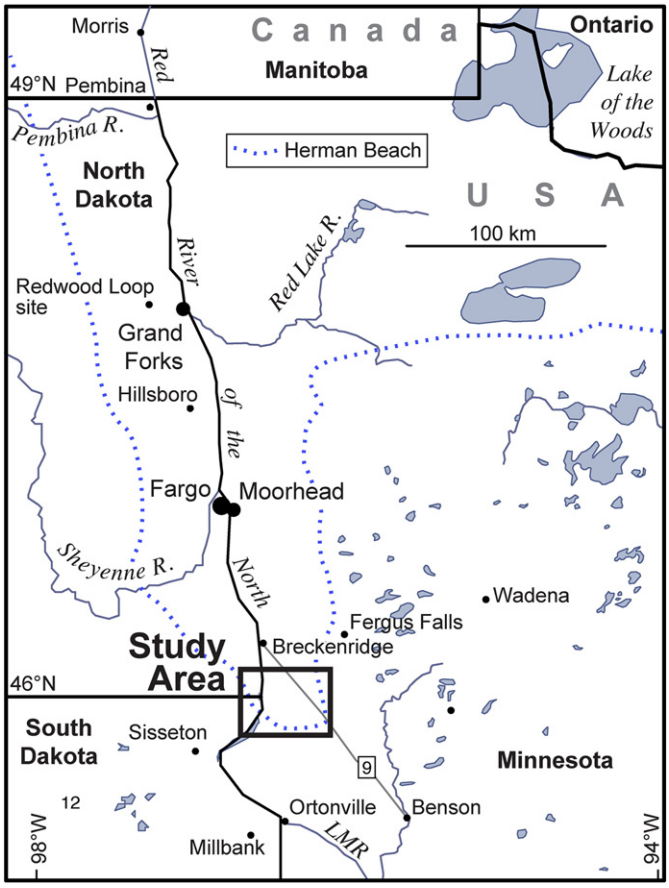

Figure 1. Location map of the southern basin of Lake Agassiz (blue dotted line) and the path of the Red River of the North. The study area is indicated by the bold rectangle at the junction of Minnesota, North Dakota and South Dakota.

1995; Teller et al., 2000) where beach materials overlie organic materials. The same stratigraphy is found some 50 km away at Swift, MN (Bjork and Keister, 1983). Collectively these sites yield three radiocarbon analyses constraining the formation of the strandline (9460 ± 90 TO-2269; 9380 ± 90 TO-4873; 9350 ± 100 WIS-1324). This indicates that the Upper Campbell strandline is younger than 10,280–10,880 cal yr BP with a probability of 0.89.

There has been recent success using OSL dating on Agassiz strandlines at the mouth of the southern outlet (Lepper et al., 2007), and west of Fargo, ND (Fig. 1) where mapping was aided by LiDAR DEMs (Lepper et al., 2011). Here we extend this methodology to the southernmost end of Lake Agassiz with a focus on the uppermost named water planes; the Herman, Norcross, Tintah and Campbell strandlines.

To put the studied strandlines into an overview context of Lake Agassiz, a brief history of the lake phases follows. See Fisher et al. (2011) for a more detailed history of the lake. Once the lake was established when the Red River Lobe of the Laurentide Ice Sheet retreated north of the Big Stone Moraine, the lake experienced three phases characterized by significant lake-level change and outlet history. The early Lockhart Phase includes formation of the Herman, Norcross, Upham and Tintah strandlines when Lake Agassiz drained south through the southern outlet (Fig. 1) to the Gulf of Mexico (Fisher, 2003). Next, the Moorhead Phase occurred when the southern outlet was abandoned and lake level fell to an unknown elevation somewhere north of Grand Forks, ND (Fig. 1). The Emerson Phase began after lake level rose in the southern basin and the southern outlet was re-occupied. The Campbell strandlines formed during the Emerson Phase. Subsequent phases of the lake were initiated following final abandonment of the southern outlet, lake-level fall, merging with glacial Lake Ojibway, and finally, drainage into Hudson Bay (Barber et al., 1999; Clarke et al., 2003).

The Herman, Norcross, Upham, Tintah and Campbell shorelines are critical to understanding the deglacial and post-glacial history of the North American mid-continent and global climate change in that they bracket at least one major reduction in the water level (Moorhead low) in Lake Agassiz and their formation (~10 ka to 14 ka) spans the time period of the Younger Dryas. Here we report the first geologic ages for Lake Agassiz strandlines obtained at field sites along the namesake transect. In addition, we present the cumulative set of OSL ages for beach deposits from several sites around the margin of the southern basin and discuss the strandline chronology in light of paleoclimate reconstructions.

Methods

LiDAR methods

The DEMs in Figures 2, 3 & 5 were constructed with bare earth model data from the International Water Institute, Red River basin mapping initiative (http://www.internationalwaterinstitute.org/lidar.htm). Approximate vertical resolution is 0.15 m with a 1 m horizontal resolution. The 2 km^2 tiles were mosaiced together using a LiDAR processing software add-on to ENVI 4.7 software. The topographic profiles (Fig. 4) and hillshade DEM images were created in ENVI, with a sun angle of 300° azimuth and 10° elevation. The LiDAR data reveals the shorelines in unprecedented detail. Here, we collectively refer to beach ridges, wave-cut scarps, and spits as strandlines (cf. Elson, 1967; Fisher, 2005; Lepper et al., 2011).

OSL methods

Sampling sites were identified as close as possible to the namesake towns based on two primary characteristics; topographic expression in field reconnaissance, and linear or elongated-ovoid soil mapping units with sandy or gravelly upper pedons (cf. Brevik, 1999). High resolution LiDAR imagery was not available to guide sample site selection, but all sample sites have been interpreted below with the new topographic information. The resulting group of sampling locations is indicated in Table 1 and Figures 2 and 3. Profiles excavated for OSL sampling are depicted in Figure 4 and the supplemental materials.

Field collection and laboratory preparation of quartz sand extracts in the grain size range 150–250 μm for OSL dating followed the methods described in the supplement to Lepper et al. (2007). OSL measurements and irradiations were conducted using a Risø DA-15 automated TL/OSL reader system. The system is equipped with a $^{90}Sr/^{90}Y$ ß-source for dose calibrations, which irradiated at a rate of 0.132 Gy/s. Luminescence was stimulated with blue light (470 ± 30 nm) from a diode array and measured with an EMI model 9235QA PMT in the UV emission range (5 mm Hoya U-340).

OSL data were collected using single-aliquot regenerative dose procedures (Murray and Wintle, 2000; Wintle and Murray, 2006). Dose–response calibration was conducted for every aliquot, and equivalent doses (D_e) were interpolated by linear local slope approximation. D_e data sets ranging in size from 94 to 110 aliquots per field sample were analyzed using the techniques outlined in Lepper et al. (2007—supplement). Except where noted, equivalent dose distributions obtained from the samples in this study were symmetric ($M/m < 1.05$) and had dose recovery fidelity (δD_c) well within acceptable limits. All samples in this study have δD_c values <2%, while samples with δD_c values as high as 5% have yielded acceptable results (Lepper et al., 2000, 2007 supplement). As such, the mean and standard error of each equivalent dose distribution was used as the basis for age calculations (with only one exception which is discussed in the Results section).

Dose rates for samples in this investigation were calculated from elemental concentrations of K, Rb, U, and Th following Aitken (1998). Elemental analysis was obtained from instrumental neutron activation (INAA) performed at the Ohio State University research reactor (Table 2). The collection depth and average water content for each

https://doi.org/10.1016/j.yqres.2013.02.002 Published online by Cambridge University Press

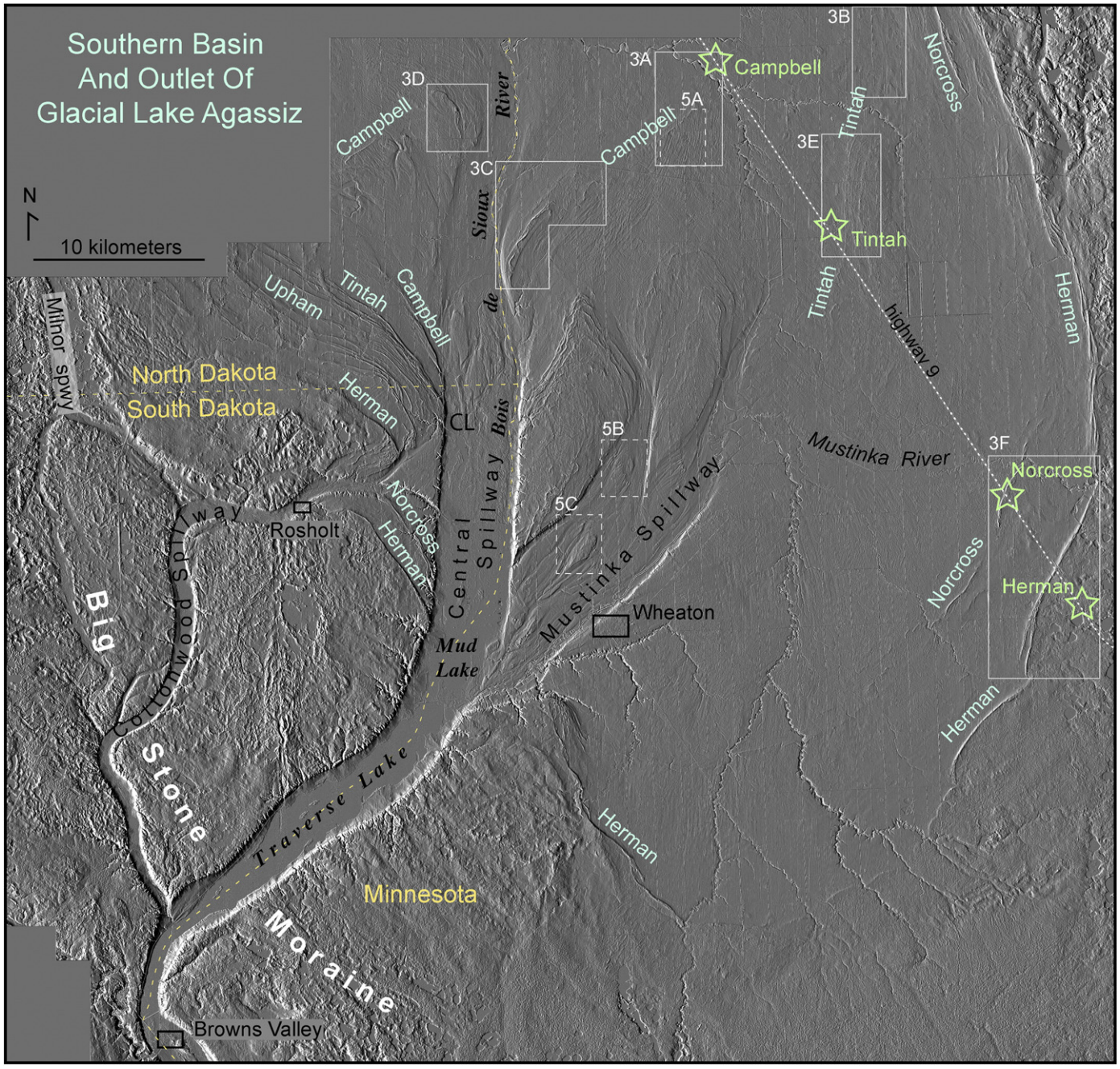

Figure 2. Hillshaded LiDAR DEM of the namesake transect and southern outlets. The namesake towns are indicated by stars and the strandlines and southern spillway channels are labeled. Locations of site specific DEMs are indicated by white polygons and labeled with figure numbers.

sample is also given in Table 2. The cosmic ray dose at depth was calculated using the equations of Prescott and Hutton (1988, 1994). The methods used are the same as those used in Lepper et al. (2007, 2011) so that results obtained from these studies are directly comparable.

The samples in this investigation exhibit a high degree of dosimetric variability (Supplemental Fig. S1; Supplemental Table S1). The lithology and stratigraphy of the strandline deposits are highly heterogeneous, so heterogeneity in the concentration and distribution of naturally occurring radioactive elements, and thereby, dosimetric variability is not unexpected. We adopted the following strategy to address this issue. If the dose rates (D′) calculated from INAA analysis of individual sub-samples are well clustered, the average of the dose rate determinations is used (e.g., 3/3) for age calculations. If the D′ determinations are separated into 2 clearly identifiable groups the average of the two grouped D′s (e.g., 2/3) are used. If all the D′ values were widely dispersed, as was the case for samples AB0708 and AB0711 the intermediate D′ value (e.g., 1/3) is used. Samples AB0802 and AB0803 come from the same sedimentary unit, therefore the average of all six available D′ determinations is used (6/6) for age calculations of these samples.

Results

LiDAR analysis and geomorphological context

The geomorphology of strandlines and spillway-floor elevations are used to reconstruct the southern outlet history. These and traces of less well-expressed strandlines are labeled on Figure 2. East of the Central Spillway, the Herman and a few Norcross strandlines are clearly evident where strandlines are expressed as wave-cut cliffs or

https://doi.org/10.1016/j.yqres.2013.02.002 Published online by Cambridge University Press

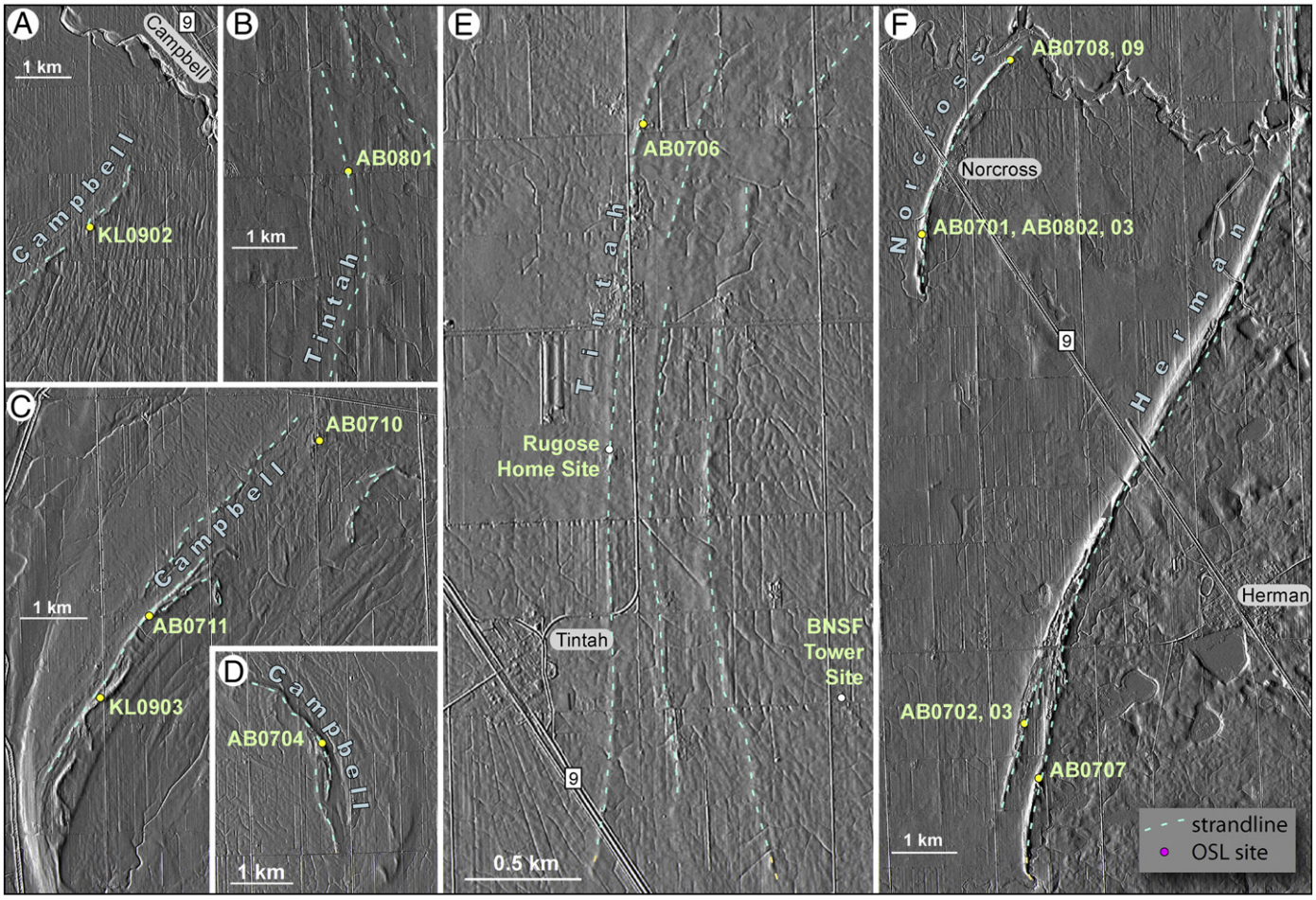

Figure 3. Larger-scale views of hillshaded LiDAR DEMs focusing on specific study sites. See Figure 2 for location of sites. Study sites are indicated by circles, and the sample numbers indicate where samples were collected.

escarpments, often with spits on their southern side. At elevations lower than the Norcross level, and at the resolution of Figure 2, strandlines are not well expressed. West of the Central Spillway, the strandlines from high to low elevations are found closer together than on the east side of the spillway. Across most of the southern basin the Herman strandline demarcates the boundary between moraine and lacustrine topography. On the western side of Figure 2, muted topography above the elevation of the Herman strandline records higher water levels previously mapped as the Milnor level (Fisher, 2005; Matsch, 1983), during which time the Milnor spillway was active. Once lake level fell to the Herman level the Cottonwood and presumably Central spillways were active. Subsequent incision of the Central Spillway below the Norcross level lead to abandonment of the Cottonwood Spillway. The Mustinka Spillway was abandoned once water levels dropped below the Tintah level. When the lake was at the Campbell level, only the Central Spillway was active.

The LiDAR hillshade DEMs reveal topographic features of the basin in detail. Here we point out the curvy lineaments evident in Figures 5A–C, consisting of parallel ridges and grooves with ~100 m widths that converge into, and are found at the northern ends of the Central and Mustinka spillways. Their formation at the mouth of the spillway (Fig. 2) is assumed to be from erosion by parallel sets of vortices in sheetflows where flow from the lake basin accelerated into the spillway. Within the Mustinka spillway, streamlined erosional remnants characteristic of flow within spillways also occur (Fisher, 2004, 2005; Kehew et al., 2009). Note that in Figures 3A & 5A, the Campbell escarpment truncates flow lineaments.

Herman ages

The Herman shoreline is well expressed in the region of the namesake transect and began developing immediately after ice withdrew from the Big Stone Moraine (Lepper et al., 2007). In this study, OSL ages were obtained from two sites approximately 4 km southwest of the town of Herman, MN from a pair of spits traceable between the sample sites and the Herman, MN airstrip (Fig. 3F; Table 1). Two samples are from the lakeward spit: AB0702 from a ripple cross-laminated fine sand, and AB0703 from a slightly deeper, weakly planar-bedded medium sand (Fig. 4 and supplement). These samples yielded ages of 14.2 ± 0.3 ka and 14.3 ± 0.3 ka, respectively. We use here the convention for reporting OSL error associated with the variability in the OSL D_e measurements, which is taken as the standard error of the OSL equivalent dose distribution divided by the dose rate (Lepper et al., 2011). Table 3 also includes the propagated age uncertainty (Aitken, 1985). The landward spit is 2 m higher than its lakeward companion, and the sample AB0707 from planar-bedded, fine sand gave an age of 14.6 ±0.3 ka. These ages could be interpreted to imply that the Herman level was occupied for at least 400 yr. Although it is sensible that the lakeward spit would be younger, the ages are indistinguishable at the ± 1 std. err. level, which also permits an interpretation that the Herman beach was occupied for much less than 400 yr.

Norcross ages

The Norcross shoreline occurs as a series of discontinuous ridges at, and adjacent to, their namesake town (Fig. 2; Table 1). The town site of

https://doi.org/10.1016/j.yqres.2013.02.002 Published online by Cambridge University Press

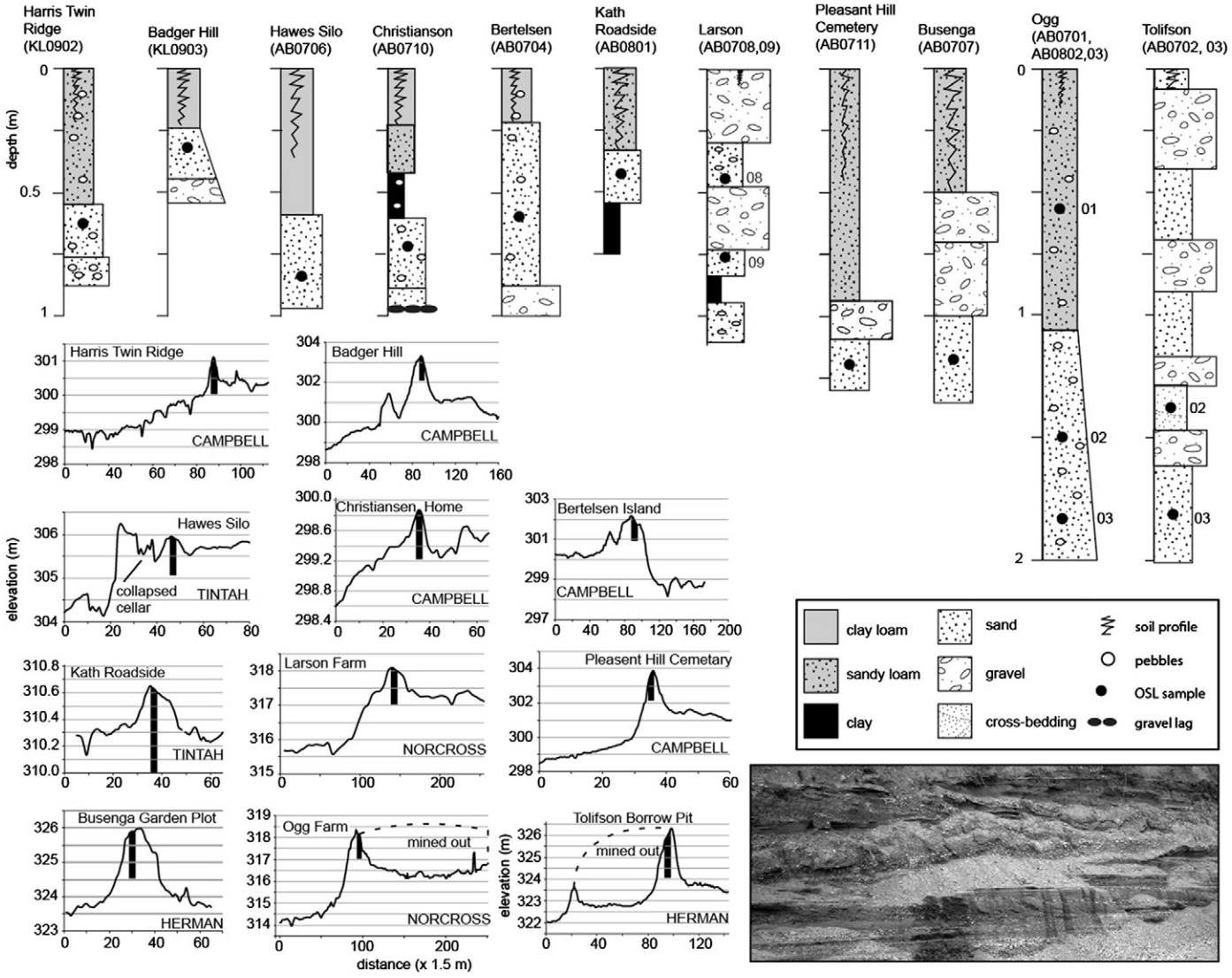

Figure 4. Simplified lithostratigraphic logs and LiDAR elevation profiles for each sample site (more detailed sediment logs are presented in the supplement). The vertical black bars on the profiles indicate the location of the respective log. The inset photo from a Norcross strandline represents typical stratification of sand and gravel beds in Lake Agassiz beach deposits.

Norcross lies on a continuous, gently arcing ridge segment extending ~2 km both to the northeast and southwest of town (Fig. 3F). Stratigraphic sets of OSL samples were collected from two sites on either side of Norcross (Fig. 4 and supplement).

Initial analyses of OSL equivalent dose (D_e) distributions for both sampled horizons at the Larson farm site exhibited characteristics that could result in poor reproducibility of OSL ages. The unfiltered D_e data sets for sample AB0708, collected from a massive, pebbly sand, and AB0709, taken from a planar-bedded fine sand (Fig. 4 and supplement), were moderately positively asymmetric with mean/median ratios of 1.06 and 1.08, respectively (M/m; Table 3), suggesting some degree of incomplete signal resetting (Lepper et al., 2007 supplement). However,

Table 1
Sampling sites.

Site name	Coordinates	Ridge elevation	Inferred ridge correlation	Samples from the site
Bertelsen Island	46° 04′ 51.59″ N; 96° 36′ 04.62″ W	302 m	Campbell	AB0704
Christianson Home Site	46° 02′ 40.06″ N; 96° 30′ 46.75″ W	301 m	Campbell	AB0710
Pleasant Hill Cemetery	46° 01′ 18.61″ N; 96° 32′ 48.85″ W	302 m	Campbell	AB0711
Harris Twin Ridge	46° 04′ 16.37″ N; 96° 25′ 54.88″ W	301 m	Campbell	KL0902
Badger Hill	46° 00′ 39.77″ N; 96° 33′ 21.58″ W	303 m	Campbell	KL0903
Hawes Silo	46° 03′ 03.53″ N; 96° 18′ 20.04″ W	307 m	Tintah	AB0706
Kath Roadside	46° 06′ 31.30″ N; 96° 16′ 40.98″ W	307 m	Tintah	AB0801
Raguse Home Site	46° 01′ 36.80″ N; 96° 18′ 37.55″ W	306 m	Tintah	*Inappropriate for sampling*
BNSF Communication Tower	46° 00′ 27.43″ N; 96° 17′ 07.89″ W	308 m	Tintah	*Inappropriate for sampling*
Ogg Farm	45° 51′ 32.28″ N; 96° 12′ 09.00″ W	318 m	Norcross	AB0701; AB0802; AB0803
Larson Farm	45° 52′ 56.81″ N; 96° 11′ 04.96″ W	318 m	Norcross	AB0708; AB0709
Tolifson Borrow Pit	45° 47′ 33.58″ N; 96° 11′ 11.20″ W	325 m	Herman	AB0702; AB0703
Busenga Garden Plot	45° 47′ 11.37″ N; 96° 11′ 01.24″ W	327 m	Herman	AB0707

https://doi.org/10.1016/j.yqres.2013.02.002 Published online by Cambridge University Press

Table 2
Average concentration of dosimetrically relevant elements from instrumental neutron activation analysis (INAA) and other dosimetric data.

Sample ID	Depth (cm)	H_2O content (%)	N_{INAA}[a]	K concentration (ppm)	Rb concentration (ppm)	Th concentration (ppm)	U concentration (ppm)	Dose rate (Gy/ka)
AB0701	56	10 ± 3	2/3	9779 ± 769	33.05 ± 4.24	2.413 ± 0.203	0.999 ± 0.106	1.382 ± 0.107
AB0702	137	12 ± 3	3/3	11438 ± 946	35.27 ± 4.46	2.082 ± 0.177	1.070 ± 0.129	1.465 ± 0.118
AB0703	182	15 ± 3	3/3	10800 ± 927	35.00 ± 3.84	2.943 ± 0.241	1.121 ± 0.123	1.430 ± 0.113
AB0704	63	10 ± 3	2/3	12039 ± 1053	45.57 ± 6.12	3.254 ± 0.270	0.684 ± 0.103	1.560 ± 0.131
AB0706	85	12 ± 3	2/3	11905 ± 950	40.80 ± 3.93	3.381 ± 0.272	2.082 ± 0.189	1.813 ± 0.132
AB0707	120	8 ± 3	3/3	10012 ± 837	33.34 ± 5.42	2.444 ± 0.208	1.047 ± 0.117	1.430 ± 0.114
AB0708	44	10 ± 3	1/3	10160 ± 838	38.01 ± 4.52	1.740 ± 0.151	0.756 ± 0.121	1.323 ± 0.112
AB0709	81	12 ± 3	2/3	10645 ± 1113	38.25 ± 7.49	2.811 ± 0.243	1.246 ± 0.136	1.497 ± 0.133
AB0710	72	15 ± 3	2/3	10503 ± 844	41.27 ± 4.46	2.408 ± 0.199	1.166 ± 0.125	1.402 ± 0.109
AB0711	120	10 ± 3	1/3	9645 ± 833	34.33 ± 3.58	2.365 ± 0.183	0.737 ± 0.132	1.296 ± 0.110
AB0801	43	12 ± 3	2/3	12155 ± 912	47.64 ± 5.93	4.824 ± 0.397	1.699 ± 0.177	1.849 ± 0.132
AB0802	150	15 ± 3	6/6	9730 ± 806	32.04 ± 4.60	2.527 ± 0.212	1.030 ± 0.111	1.300 ± 0.102
AB0803	182	15 ± 3	6/6	9730 ± 806	32.04 ± 4.60	2.527 ± 0.212	1.030 ± 0.111	1.294 ± 0.101
KL0902	66	15 ± 3	1/1	15268 ± 1213	47.90 ± 3.20	2.555 ± 0.243	0.861 ± 0.113	1.730 ± 0.140
KL0903	33	10 ± 3	1/1	11108 ± 950	35.62 ± 2.42	4.257 ± 0.383	0.533 ± 0.088	1.518 ± 0.124

See supplemental materials for full data sets.
[a] Number of INAA analyses used for dose rate calculation/number of independent INAA analyses performed. Selection criteria discussed in the text.

after data filtering (as described in Lepper et al., 2003, 2007) both D_e data sets became symmetric (M/m values < 1.05). Because of this potential discrepancy, entirely new OSL data sets were collected: AB0708a and AB0709a (Table 3). In the case of sample AB0708a the D_e data set was positively asymmetric before and after filtering so the sample was treated as incompletely reset for age calculation (Lepper and McKeever, 2002; Lepper et al., 2007 supplement). The OSL age determined for AB0708a was 13.6 ± 0.3 ka, while AB0709a from lower in the profile yielded an age of 16.2 ± 0.2 ka.

At the Ogg farm site, south of Norcross, two entirely separate OSL data sets from the same field sample, AB0701 and AB0701a, yielded ages of 13.3 ± 0.3 ka and 13.6 ± 0.3 ka, indistinguishable within error limits. Two separate data sets were collected to maintain consistency with the Larson farm site and to verify reproducibility of the ages. Samples AB0802 and AB0803 were collected lower in the Ogg farm profile, but both from within the same gravelly sand unit (Fig. 4 and supplement). Ages of 15.4 ± 0.3 ka and 15.9 ± 0.3 ka, respectively, were obtained from these samples. The correspondence between these ages and the age of 16.2 ± 0.3 ka from sample AB0709a, at the Larson Norcross site is intriguing and is discussed further below.

The three ages from the lowest stratigraphy at the Norcross sites (16.2 ± 0.3 ka, 15.4 ± 0.3 ka, 15.9 ± 0.3 ka; Fig. 5A) are all older than the ~14.2 ka age for the Big Stone Moraine (Lepper et al., 2007). Moreover, these ages are indistinguishable from the Bemis Moraine (16.25 ka cal BP—Lowell et al., 1999) and the re-advance to the Algona Moraine (15.1 ka cal BP—Ruhe, 1969; Bettis et al., 1996). The Bemis and Algona moraines formed by the same ice lobe as the Big Stone Moraine, and are 450 and 300 km down ice, respectively. Because it is highly unlikely to deposit sand and gravel associated with a shoreline beneath the glacier when the frontal ice-margin position is 450 km away, the dates are not taken here to reflect the age of the strandline sediment. Instead, these ages could be interpreted to suggest: (1) that in the early stages of formation of the Norcross beach wave and/or storm energy was strong and created high turbidity conditions in the littoral zone that prevented proper resetting of the sediments that now form the lower portion of the Norcross beach profiles; (2) that dose rate-heterogeneity in the lower Norcross stratigraphy was not resolved; or, (3) these ages could indicate supraglacial exposure of sand at the ice surface before deposition through a crevasse or moulin into a subglacial relic or buried landform, that served as a core for the exceptionally well-expressed strandline segment at Norcross, MN.

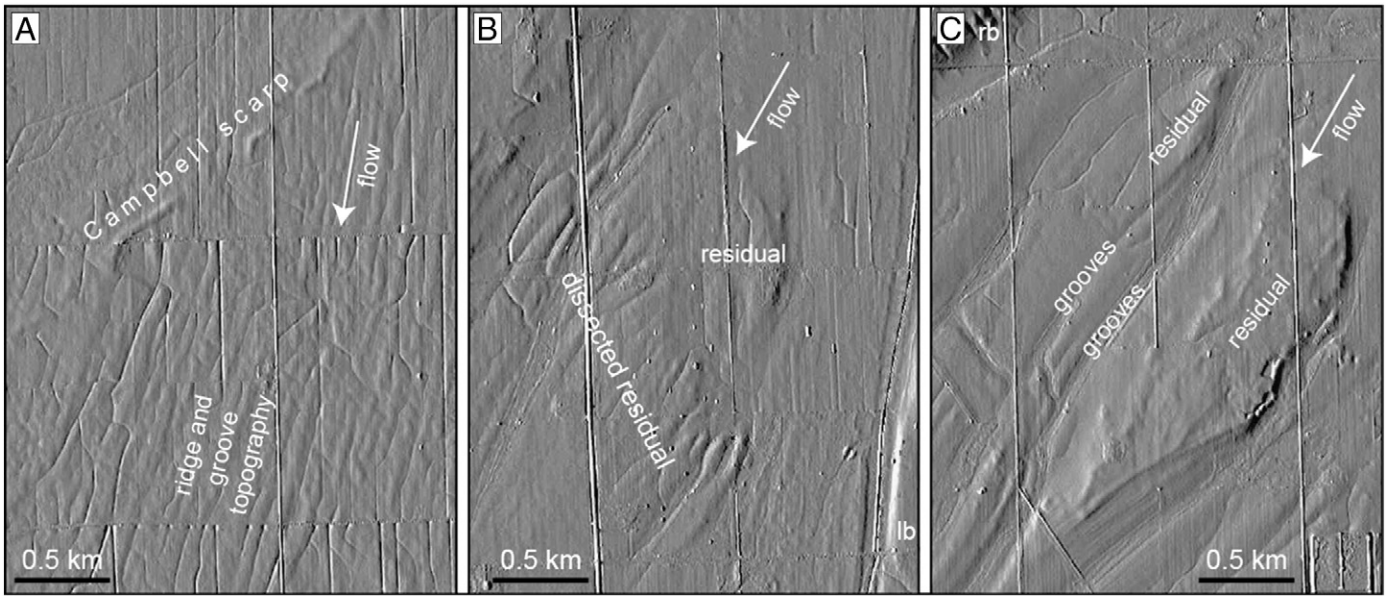

Figure 5. Hillshaded LiDAR DEMs reveal erosion in the spillway channel as ridge and grooved topography at (A) the head of the Mustinka spillway channel, and also as formation of streamlined residual forms (B, C) within the Mustinka spillway channel.

https://doi.org/10.1016/j.yqres.2013.02.002 Published online by Cambridge University Press

Table 3
OSL age results and related data.

Sample ID	Beach name	Sample depth (cm)	N_{De}[a]	δ D_c[b]	M/m (all data)	M/m (filtered)	Equivalent dose[c] (Gy)	Dose rate (Gy/ka)	Age[d] (ka)
AB0704	Campbell	63	92/96	0.2%	1.01	0.99	16.681 ± 0.415	1.560 ± 0.131	10.7 ± 0.3 (0.9)
KL0902	Campbell	66	95/95	0.8%	1.00	n/a	18.299 ± 0.365	1.730 ± 0.140	10.6 ± 0.2 (0.9)
KL0903	Campbell	33	93/95	1.0%	1.00	1.01	16.171 ± 0.346	1.518 ± 0.124	10.7 ± 0.2 (0.9)
AB0710	Campbell	72	94/96	0.4%	1.01	1.01	16.853 ± 0.428	1.402 ± 0.109	12.0 ± 0.3 (1.0)
AB0711	Campbell	120	92/96	0.4%	1.02	1.01	17.630 ± 0.393	1.296 ± 0.110	13.6 ± 0.3 (1.1)
AB0801	Tintah	43	92/96	1.4%	1.00	0.99	15.850 ± 0.340	1.849 ± 0.132	8.6 ± 0.2 (0.6)
AB0706	Tintah	85	93/96	0.9%	1.03	1.01	20.847 ± 0.403	1.813 ± 0.132	11.5 ± 0.2 (0.9)
AB0701	Norcross	56	108/110	0.4%	0.98	0.98	18.748 ± 0.290	1.382 ± 0.107	13.6 ± 0.2 (1.1)
AB0701a	Norcross	56	96/96	1.0%	1.00	n/a	18.427 ± 0.358	1.382 ± 0.107	13.3 ± 0.3 (1.1)
AB0708	Norcross	44	93/96	0.4%	1.06	1.04	–	–	–
AB0708a	Norcross	44	92/95	0.5%	1.14	1.08	17.995 ± 0.457[c]	1.323 ± 0.112	13.6 ± 0.3 (1.2)
AB0709	Norcross	81	93/96	1.4%	1.08	1.04	–	–	–
AB0709a	Norcross	81	93/96	1.0%	1.03	1.02	24.278 ± 0.459	1.497 ± 0.133	16.2 ± 0.3 (1.5)
AB0802	Norcross	150	95/96	1.4%	1.01	1.00	20.002 ± 0.353	1.300 ± 0.102	15.4 ± 0.3 (1.2)
AB0803	Norcross	182	94/96	0.6%	1.01	1.02	20.619 ± 0.414	1.294 ± 0.101	15.9 ± 0.3 (1.3)
AB0702	Herman	137	93/96	0.4%	1.02	1.00	20.806 ± 0.417	1.465 ± 0.118	14.2 ± 0.3 (1.2)
AB0703	Herman	182	95/96	1.7%	1.00	1.00	20.520 ± 0.305	1.430 ± 0.113	14.3 ± 0.2 (1.2)
AB0707	Herman	120	94/96	1.5%	1.04	1.01	20.852 ± 0.458	1.430 ± 0.114	14.6 ± 0.3 (1.2)

a) Sample reprocessed and an entirely new set of OSL equivalent dose data collected.
[a] Number of aliquots used for OSL D_e calculation/number of aliquots from which OSL data was collected.
[b] Dose recovery fidelity (refer to "check dose" in Lepper et al., 2000 and supplement to Lepper et al., 2007).
[c] Equivalent doses are the mean and standard error of the OSL De distributions, except in the case of the asymmetric, filtered data set obtained from sample AB0708a where the "leading edge" D_e and modified standard error were used (see Supplement to Lepper et al., 2007).
[d] Presented as calculated OSL age ± std. err. (uncertainty); convention proposed in Lepper et al., 2011.

Tintah age and atypical stratigraphy

The Tintah shoreline occurs as a set of three-to-five, faintly-expressed linear, to gently arcing undulations, just east of the town of Tintah, MN, and extending ~6 km north of the town site (Fig. 3E). Of the four sites explored for sampling, only two were sampled (Table 1). At all sites, sedimentary profiles were atypical of other Lake Agassiz strandline deposits. Three of the sites—Hawes silo, BNSF communication tower, and Raguse home site—exhibited clay overlying relatively thin sands or gravels (Supplement). At the Raguse home site, a thin lag of pebbly sand and cobbles overlies diamicton. Although not ideal, a sample was collected from a coarse sand horizon at the Hawes Silo site (AB0706; Fig. 3E). The Kath roadside site was distinct from the other Tintah sites examined. Below a sand-rich organic soil horizon, 33 cm of highly uniform, very-fine sand overlying clay was sampled (AB0801; Fig. 4 and supplement). These samples yielded OSL ages of 11.5 ± 0.2 ka for AB0706 and 8.6 ± 0.2 ka for AB0801 (Table 3). Later examination of images derived from LiDAR data indicates a crescent-shaped landform at the Kath Roadside site. We interpret the age of 8.6 ± 0.2 ka from sample, AB0801, to reflect post-lake eolian dune migration.

Campbell ages

The Campbell shorelines are generally cited as being the most well expressed, and as being traceable for the greatest distances in the Lake Agassiz basin. In that context it is noteworthy that the Campbell shoreline is not expressed at the town site of Campbell, MN. However, shorelines in this area generally trend southwestward toward the southern outlet and this trend in shoreline segments can be traced to the Campbell town site. Based on morphological orientation and ridge elevations between 301 and 303 m, four sites in Minnesota and one in North Dakota, across the Bois de Sioux River in the Central Spillway, were identified for sampling ranging from approximately 4 to 16 km from the town of Campbell (Fig. 2; Table 1).

The dating results are presented as younger and older clusters. Starting with the younger cluster, sample KL0902 was collected from faintly planar-bedded, medium sand within a low-relief ridge atop an arcuate, north facing escarpment cut into ridge and groove terrain, ~3 km southwest of the Campbell town site (Figs. 3A; 4 and supplement). The age obtained for the sample was 10.6 ± 0.2 ka. Sample KL0903 was collected from a thinly-laminated medium sand within a sinuous ridge atop the Campbell scarp (Figs. 3C; 4) and yielded an age of 10.7 ± 0.2 ka. Across the Central Spillway in North Dakota, sample AB0704 was collected from faintly planar-bedded coarse sand overlying gravel. This is within the lakeward beach ridge or spit pair that gave the appearance of an island from ground level (Figs. 3A; 4 and supplement). An age of 10.7 ± 0.3 ka was obtained. These three ages agree well with other radiocarbon and OSL ages for the Campbell strandline (Bjork and Keister, 1983; Lepper et al., 2011; Risberg et al., 1995; Teller et al., 2000).

In the older cluster there are two sample sites. Sample AB0710 was collected from a low-relief hillock along the trend of the Campbell strandline that appears to be situated landward of the primary strandline at this location (Fig. 3C). In this area shorelines are discontinuous, expressed as isolated scarps and very-low relief ridges. The stratigraphy at this location again reveals a clay layer over the medium sand, beach-like deposit (Fig. 4 and supplement). The age obtained from sample AB0710 was 12.0 ± 0.3 ka. Further to the southwest, the Campbell shoreline forms a prominent scarp with three sinuous ridge segments perched atop of it (Fig. 3C). Sample AB0711 from the Pleasant View Cemetery was collected from a relatively deep position, consisting of fine sand overlain by a pebbly sand layer at the crest of the scarp (Fig. 4 and supplement). The age determined was 13.6 ± 0.3 ka. At this site the scarp does not appear to be overlain by a ridge segment. It is possible that the age obtained reflects an older stratigraphy, and that the scarp is not mantled with Campbell-aged deposits, or that we excavated through Campbell-aged sediments at this site (see supplement). These two ages are older than the established Campbell strandline age.

Discussion

Just as LiDAR imagery is revolutionizing mapping of low-relief strandlines in the Agassiz basin, the OSL dating method has become the technique-of-choice in light of the absence of organics for radiocarbon dating within littoral deposits of Lake Agassiz. Since most field sampling was completed before LiDAR imagery was available, not all resulting OSL ages could be simply assigned to the strandlines. Five dates in particular were older than expected. These inconsistent ages were discussed in the preceding results section and are not included in the following age assignments for water planes of the Lockhart Phase.

https://doi.org/10.1016/j.yqres.2013.02.002 Published online by Cambridge University Press

Table 4
Compilation of OSL ages for beach ridges correlated to the Herman, Norcross, Upham, and Campbell complexes.

Site	Sample	Grain size	M/m	Elevation (m)	Published age (ka)	Std err of age (ka)	Uncert. (ka)	Source
Ridges correlated to Herman								
Rosholt pit	KL0505	VFS-FS	1.02	325	13.6	0.4	1.4	Lepper et al., 2007
Emden mammoth	KL0901LS	FS	1.02	334	14.0	0.3	1.2	Lepper and Sager, 2010
Rosholt pit	KL0506	FS	1.02	325	14.0	0.3	1.2	Lepper et al., 2007
Rosholt pit	KL0506	VFS	1.03	325	14.2	0.3	1.2	Lepper et al., 2007
Wheatland, ND transect	KG0504	FS	1.00	335	14.1	0.2	1.3	Lepper et al., 2011
Wheatland, ND transect	KG0504	VFS	1.00	335	14.3	0.2	1.3	Lepper et al., 2011
Tolifson borrow pit	AB0702	FS	1.00	325	14.2	0.3	1.2	This manuscript
Tolifson borrow pit	AB0703	FS	1.00	325	14.3	0.3	1.2	This manuscript
Busenga garden plot	AB0707	FS	1.01	327	14.6	0.3	1.2	This manuscript
	Mean				**14.1**	0.3	1.2	
	Std dev				**0.3**			
Ridges correlated to Norcross								
Wheatland, ND transect	*KG0503*	*FS*	*1.01*	*325*	*12.6*	*0.3*	*1.2*	Lepper et al., 2011
Ogg Farm	AB0701a	FS	1.00	318	13.3	0.3	1.1	This manuscript
Wheatland, ND transect	KG0503	VFS	1.00	325	13.6	0.3	1.3	Lepper et al., 2011
Ogg Farm	AB0701	FS	0.98	318	13.6	0.2	1.1	This manuscript
Larson Farm	AB0708a	FS	1.08[a]	318	13.6	0.3	1.2	This manuscript
Hudderite pit	KL0507	VFS-FS	1.05[a]	318	13.7	0.4	1.4	Lepper et al., 2007
	Mean				**13.6**	0.3	1.2	
	Std dev				**0.2**			
Ridges Correlated to Upham								
Cell phone ridge	KL0602	VFS	1.09[a]	310	13.4	0.6	1.4	Lepper et al., 2007
Boisberg pit	KL0508	VFS-FS	1.05[a]	311	13.5	0.6	1.6	Lepper et al., 2007
Double spit	KL0601	FS	1.01	314	13.5	0.2	1.2	Lepper et al., 2007
	Mean				**13.5**	0.5	1.4	
	Std dev				**0.1**			
Ridges correlated to Campbell								
Wheatland, ND transect	KG0505	FS	1.01	299	10.0	0.2	0.9	Lepper et al., 2011
Wheatland, ND transect	KG0505	VFS	1.02	299	10.3	0.2	0.9	Lepper et al., 2011
Harris twin ridge	KL0902CC	FS	1.00	301	10.6	0.2	0.9	This manuscript
Bertelsen Island	AB0704	FS	0.99	302	10.7	0.3	0.9	This manuscript
Badger Hill	KL0903CC	FS	1.01	303	10.7	0.2	0.9	This manuscript
Christianson home site	*AB0710*	*FS*	*1.01*	*301*	*12.0*	*0.3*	*1.0*	*This manuscript*
Pleasentview Cemetery	*AB0711*	*FS*	*1.01*	*302*	*13.6*	*0.3*	*1.1*	*This manuscript*
	Mean				**10.5**	0.2	0.9	
	Std dev				**0.3**			

Samples in italics are those not included in the calculation of the mean.
[a] Leading edge method used for samples with M/m ≥ 1.05.

OSL age assignments for Lake Agassiz strandlines

The new ages provide a chronology for Lake Agassiz shorelines along the transect where Warren Upham assigned their names during his work in the 1890's. The three OSL ages at Herman, MN average to 14.4 ± 0.3 ka, which is consistent with the glacial ice-recession age from the Big Stone Moraine within reported errors (Lepper et al., 2007). The three OSL ages from the upper beach profiles at Norcross, MN yielded an average of 13.5 ± 0.3 ka. A single age, from a deposit atypical of Agassiz beaches, of 11.5 ± 0.2 ka was obtained at Tintah, MN. And, three robust ages from the area of Campbell, MN gave an average of 10.7 ka ± 0.2 ka.

The significance of these new ages is magnified by incorporating them into a growing OSL age data set, which produces a highly consistent chronology for four of the five recognized strandline complexes (Table 4). Nine ages from five separate field areas separated by more than 150 km have now been reported for strandlines correlated to the Herman (Table 4). The mean and std. dev. of these published ages is 14.1 ± 0.3 ka. The average std. err. of these ages is also 0.3 ka. The strong correspondence between inter-sample standard deviation and intra-sample standard error provides additional validation for the error reporting method that was proposed by Lepper et al. (2011) for OSL SAR data sets containing equivalent doses (D_es) measured from a large number of aliquots (n = ~100).

Strandlines correlated to the Norcross have yielded six ages from four different field sites (Table 4). Excluding the anomalously low value of 12.6 ka from the Wheatland transect (Lepper et al., 2011), the mean and std. dev. of the ages is 13.6 ± 0.2 ka with an average std. err. of 0.3 ka.

Three Upham strandline ages from three separate sites, including a spit, were collected from the head of the central spillway where Fisher (2005) defined the Upham level (Table 4). The mean and std. dev. of the ages is 13.5 ± 0.1 ka with an average std. err. of 0.5 ka (Lepper et al., 2007).

The age of the Tintah strandline complex remains unresolved. Our explorations near Tintah, MN revealed deposits that were atypical of those seen in the other three major beach complexes. In the study area three Tintah strand sites exhibited pebbly-clay horizons overlying sands and/or had horizons that could be interpreted as lags (Supplement). The singular Tintah age obtained in this study was 11.5 ± 0.2 ka, however, an age of 12.0 ± 0.3 ka was also obtained from a ridge segment slightly landward of the Campbell strand. Additionally, ages of 11.3 ± 0.2 ka and 12.1 ± 0.3 ka (KG0501, Lepper et al., 2011) were obtained from sands overlying a lag deposit within an uncorrelated strandline near Wheatland, ND. This set of ages broadly corresponds to the start of the Moorhead low-water Phase when the southern outlet was abandoned (Fisher and Lowell, 2006) and the southern shoreline of Lake Agassiz regressed to north of Grand Forks, ND (Fig. 1). Therefore we interpret

https://doi.org/10.1016/j.yqres.2013.02.002 Published online by Cambridge University Press

these ages to reflect other, non-littoral sedimentary processes acting on the subaerial landscape in the southern basin. Currently, the best candidate for a Tintah strandline age remains the beach deposits of the "310 m strandline" from the Wheatland transect (Lepper et al., 2011) with provisional ages of 13.6 ± 0.2 ka (KL1004 vfs) and 13.4 ± 0.3 ka (KL1004 fs). Additional work is needed to better understand the nature and age of Tintah strandlines and deposits.

Seven ages have been obtained from six strandlines correlated to the Campbell (Table 4). Excluding the ages from AB0710 and AB0711 for reasons discussed earlier in this paper, the mean age and std. dev. is 10.5 ± 0.3 ka and the average std. err. of 0.2 ka. Traditionally, the Campbell strandline has been divided into Upper and Lower strandlines, both graded to the southern outlet, and the elevation difference between them increasing to the north (Fisher, 2005). Based on examination of Table 4 there is the possibility that the Campbell ages are bimodal, with the Upper Campbell having been sampled near Campbell, MN and yielding ages of 10.6 to 10.7 ka (this paper). While at Wheatland, ND two separate Campbell ridge segments are expressed, and the sampled lakeward scarp face is likely equivalent to the Lower Campbell and yielded an age of 10.0 to 10.3 ka (Lepper et al., 2011: Fig. 2A). Additional work, with the strategy of identifying field sites where both Campbell strandlines could be sampled, is needed to test this assertion. However, these ages can be interpreted to suggest that the Campbell strandline complex formed over a period of ~700 yr).

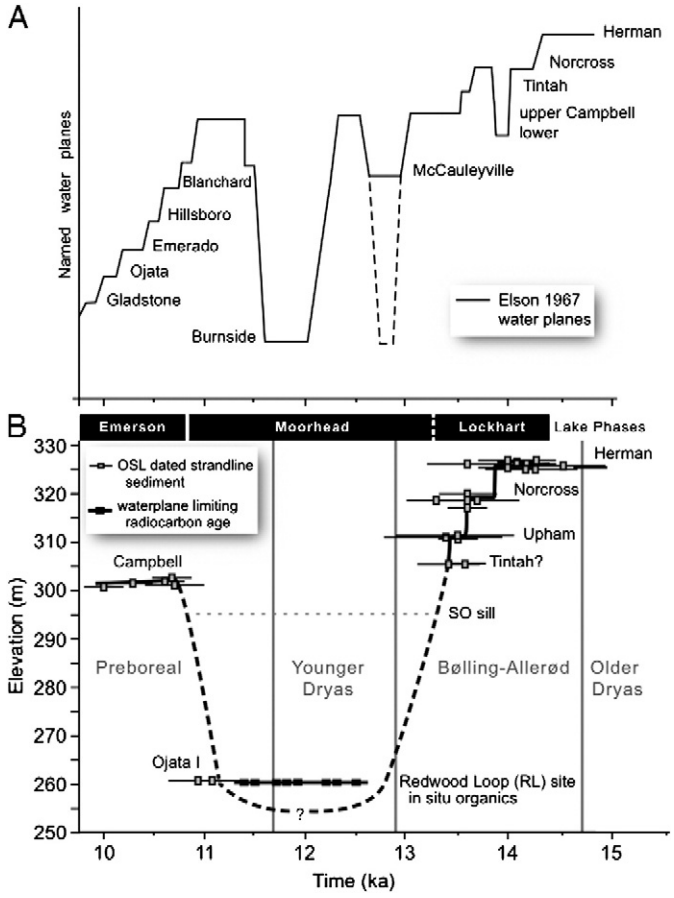

Figure 6. (A) Elson's early synthesis of lake-level history for glacial Lake Agassiz (adapted from Elson, 1967). See the supplemental materials for a re-examination of the context of the radiocarbon ages used by Elson. (B) Plot of the available OSL ages that directly date littoral sediments from the southern basin of Lake Agassiz (ages from Lepper et al., 2007, 2011; this study). With this technique of dating the strandline sediment itself, actual water plane ages are being used to generate a lake-level curve. Note that in situ organic materials buried by littoral deposits are important data points on the curve. The plotted in situ terrestrial samples from the Redwood Loop site (Fig. 1, Fisher et al., 2008) require water levels below the site's elevation. The OSL dated Ojata 1 strandline deposits overlying drowned in situ terrestrial deposits at the Redwood Loop site record the subsequent transgression. SO refers to southern outlet sill.

Lake-level history in the southern basin

The benefits of having age assignments for the strandlines are manifold. (1) Assuming accurate tracing of water planes in a proglacial lake, the northern extent of the strandline records the ice margin position at that time, in lieu of a dated moraine. (2) Strandline ages can be extended northward into a more rapidly rebounding basin, providing age constraints for the escalating number of ridges northwards. (3) Absolute rates of lake-level lowering become possible and such rates offer insight into mechanisms of lake-level lowering.

The greatest duration between successive strandlines is between the Herman and Norcross levels. In the southern basin the Herman and Norcross are arguably the strongest-developed strandlines, consisting of large scarps, spits and ridges. A histogram of strandline aggregate length plotted against elevation in five-foot (~1.5 m) intervals for the southern end of the lake basin (Fisher, 2005: Fig. 7) revealed stronger modes associated with the Herman and Norcross strandlines than for younger strandlines. This suggests a longer period of time for development for the Herman and Norcross, with constant lake levels. After the Norcross, the Upham strand has ages with standard deviations overlapping with the Norcross ages and the potential ages for the Tintah are widely dispersed. The available geomorphology and age control strongly suggests that the Upham and Tintah water planes were short-lived and younger than the Herman and Norcross levels. Fisher's (2005) histogram analysis also revealed weaker modes associated with the Tintah and Upham water planes, further supporting a shorter duration of time available for them to develop.

In conjunction with rates of lake-level fall, previous mapping of strandlines northwards along the western shore of Lake Agassiz indicates that the Herman strandlines extend north into Canada (Elson, 1967; Johnston, 1946), and the Norcross and Tintah strandlines have been mapped only a little farther (cf. Fisher and Lowell, 2012). Thus the spatial extent of strandlines is in agreement with the OSL ages, indicating that the ice margin did not retreat much farther north as lake level was falling below the Norcross level to the Tintah level. The simplest explanation for the Upham and Tintah levels is episodic incision of the spillway rather than variation in water supply alone.

An important finding from this study is that the Tintah strandline deposits are unlike those of other Lake Agassiz strandlines. This is the third study in which we have been mostly unsuccessful in obtaining a Tintah strandline age, which likely reflects a more complex formation history than would be associated with a simple static shoreline. At its namesake town, the Tintah strandline appears to be a series of low-relief scarps and ridges with minimal littoral sediments. Fisher (2005) also observed few strandlines between the Tintah and Campbell levels. Along the Wheatland transect west of Fargo, Lepper et al. (2011) noted a lack of strandlines between the 310 m ridge (possible Tintah ridge) and the Campbell strandline(s). The lack of strandlines could be explained in a variety of ways, presented here in order of increasing complexity: (1) rapid lake-level fall from the Tintah to below the Campbell level; (2) a colder climate and a much longer season of ice cover; (3) lower foreshore slopes negating littoral processes in the nearshore; or (4) some combination of the above with other factors not yet considered.

After abandonment of the Tintah strandlines, lake level fell below the southern outlet sill (SO sill, Fig. 6) marking the beginning of the Moorhead Phase. The water level fell below the elevation of the in-situ terrestrial organics recovered at the Redwood Loop site (Figs. 1, 6). Deposition of the littoral deposits buried the in situ organics at the Redwood Loop site (Fisher et al., 2008) during the transgression in the later half of the Moorhead Phase. The transgression ended when the water level rose above the southern outlet sill to the Campbell strandlines.

https://doi.org/10.1016/j.yqres.2013.02.002 Published online by Cambridge University Press

Paleoclimatic implications

When the strandline ages are considered within the context of paleoclimate indicators, an interesting pattern may be present (Fig. 6). For example, formation of the Herman, Norcross, Upham and Tintah strandlines correspond to times generally accepted to be warm as expressed in the Greenland ice-core records. The Herman appears at the start of Bølling–Allerød (BA) warming (Lowe et al., 2008), and the Norcross forms some 600 yr later, also during the warm BA interval. The cooling at the end of the BA leading into the Younger Dryas corresponds to the time when lake level was falling. Water levels remained low during the duration of the Younger Dryas but then rose. The rising water levels reached the Campbell ca. 1000 yr after the end of the Younger Dryas during the early Holocene. Although in general the strandlines formed in warmer times, the apparent lack of strandline formation during times of cold may reflect a host of factors—changing water levels, lower water levels in the basin, increased duration of winter lake ice, among others. Although work is needed to define the exact influence of climate on changes in water level in the Agassiz basin, it may be that the relationships noted here could provide a framework for future investigation.

Conclusions

Ages constraining the timing of Lake Agassiz shoreline development have been sparse and have previously not been obtained from sites near the namesake towns in the vicinity of the southern outlet. Our current work from 11 sampling sites along Upham's namesake transect has yielded 16 independent ages. The current results combined with a growing OSL age data set for Lake Agassiz's southern basin provide robust age constraints for the Herman, Norcross and Campbell strandlines with averages and standard deviations of 14.1 ± 0.3 ka, 13.6 ± 0.2 ka, and 10.5 ± 0.3 ka, respectively. The average age for the Herman strandline complex is consistent with ice withdrawal from the Big Stone Moraine and the average age of the Campbell strandline complex is consistent with existing radiocarbon age constraints. Additionally, our results suggest that the Herman, Norcross and Campbell strandline complexes may represent the only relatively stable water levels of Lake Agassiz before 10 ka.

Our observations of Tintah correlated strandline deposits in the area of the namesake transect indicate clearly different stratigraphic and sedimentological characteristics from the Herman, Norcross, and Campbell beach deposits. Only one potential Tintah age of 11.5 ± 0.2 ka was determined in this study. Three previously obtained ages for the Upham shoreline have an average and standard deviation of 13.5 ± 0.1 ka, however, this is indistinguishable from the average age for the Norcross complex. These two strandline complexes, Tintah and Upham, appear to represent more transient water levels. However, additional work is needed to better constrain their ages and to better understand the nature and formation processes of the Tintah strands in the southern basin of Lake Agassiz.

This work further emphasizes the utility of OSL dating to obtain vital chronological data for Lake Agassiz strandline deposits, which have been historically difficult to date. Additionally, this study shows the need for comprehensive integration of geomorphological, sedimentological, and geochronological analyses when working with complex climatically-linked systems such as Lake Agassiz and its shorelines.

Acknowledgments

The authors thank the Comer Science and Education Foundation for support that made work in the Lake Agassiz basin possible. We are also grateful for the encouragement offered by Wally Broecker and Richard Alley. INAA was performed at The Ohio State University Research Reactor for which the authors would like to acknowledge the efforts of Joe Talnagi. Partial support for INAA was obtained through the DOE Reactor Sharing Grant Program. Kirk Zmijewski (UT) processed the LiDAR DEM imagery and Chad Crotty (NDSU) assisted in the field.

Appendix A. Supplementary data

Supplementary data to this article can be found online at http://dx.doi.org/10.1016/j.yqres.2013.02.002.

References

Aitken, M.J., 1985. Thermoluminescence Dating. Academic Press, London (359 pp.).
Aitken, M.J., 1998. An Introduction to Optical Dating: The Dating of Quaternary sediments by the Use of Photon-stimulated Luminescence. Oxford University Press, New York (267 pp.).
Barber, D.C., Dyke, A., Hillaire-Marcel, C., Jennings, A.E., Andrews, J.T., Kerwin, M.W., Bilodeau, G., McNeely, R., Southon, J., Morehead, M.D., Gagnon, J.M., 1999. Forcing of the cold event of 8,200 years ago by catastrophic drainage of Laurentide lakes. Nature 400, 344–348.
Bettis III, E.A., Quade, D.J., Kemmis, T.J., 1996. Hog, Bogs, and Logs: Quaternary Deposits and Environmental Geology of the Des Moines Lobe. Iowa Geological Survey Guidebook Series, 18 (170 pp.).
Bjork, S., Keister, C.M., 1983. The Emerson Phase of Lake Agassiz, independently registered in northwestern Minnesota and northwestern Ontario. Canadian Journal of Earth Sciences 20, 1536–1542.
Brevik, E.C., 1999. Improved mapping of the Lake Agassiz Herman strandline by integrating geological and soil maps. Journal of Paleolimnology 22, 253–257.
Clarke, G., Leverington, D., Teller, J., Dyke, A., 2003. Superlakes, megafloods, and abrupt climate change. Science 301, 922–923.
Elson, J.A., 1967. Geology of Glacial Lake Agassiz. In: Mayer-Oakes, W.J. (Ed.), Life, Land and Water. University of Manitoba Press, Winnipeg, pp. 37–96.
Elson, J.A., 1983. Lake Agassiz—Discovery and a Century of Research. In: Teller, J.T., Clayton, L. (Eds.), Geological Association of Canada Special Paper, 26. University of Toronto Press, pp. 21–41.
Fisher, T.G., 2003. Chronology of glacial Lake Agassiz meltwater routed to the Gulf of Mexico. Quaternary Research 59, 271–276.
Fisher, T.G., 2004. River Warren boulders: paleoflow indicators in the southern spillway of glacial Lake Agassiz. Boreas 33, 349–358.
Fisher, T.G., 2005. Strandline analysis in the southern basin of glacial Lake Agassiz, Minnesota and North and South Dakota, USA. Geological Society of America Bulletin 117, 1481–1496.
Fisher, T.G., Lowell, T.V., 2006. Questioning the age of the Moorhead Phase in the glacial Lake Agassiz basin. Quaternary Science Reviews 25, 2688–2691.
Fisher, T.G., Lowell, T.V., 2012. Testing northwest drainage from Lake Agassiz using extant ice margin and strandline data. Quaternary International 260, 106–114.
Fisher, T., Yansa, C., Lowell, T., Lepper, K., Hajdas, I., Ashworth, A., 2008. The chronology, climate, and confusion of the Moorhead Phase of Glacial Lake Agassiz: new results from the Ojata beach, North Dakota, USA. Quaternary Science Reviews 27, 1124–1335.
Fisher, T.G., Lepper, K., Ashworth, A.C., Hobbs, H.C., 2011. Southern Outlet and Basin of Glacial Lake Agassiz. In: Miller, J.D., Hudak, G.J., Wittkop, C., McLaughlin, P.I. (Eds.), Archean to Anthropocene: Field Guides to the Geology of the Mid-Continent of North America: Geological Society of America, Boulder, CO, no. 24, pp. 379–400.
Johnston, W.A., 1946. Glacial Lake Agassiz, with special reference to the mode of deformation of the beaches. Geological Survey of Canada Bulletin 7, 20.
Kehew, A.E., Lord, M., Kozlowski, A.L., Fisher, T.G., 2009. Proglacial megaflooding along the margins of the Laurentide Ice Sheet. In: Burr, D., Carling, P.A., Baker, V.R. (Eds.), Megaflooding on Earth and Mars. Cambridge University Press, New York, pp. 104–127 (Ch. 7).
Lepper, K., McKeever, S.W.S., 2002. An objective methodology for dose distribution analysis. Radiation Protection Dosimetry 101, 349–352.
Lepper, K., Sager, L., 2010. A revised age determination for the Embden, North Dakota mammoth using optically stimulated luminescence dating. Current Research in the Pleistocene 27, 171–173.
Lepper, K., Agersnap-Larsen, N., McKeever, S.W.S., 2000. Equivalent dose distribution analysis of Holocene eolian and fluvial quartz sands from Central Oklahoma. Radiation Measurements 32, 603–608.
Lepper, K., Wilson, C., Gardner, J., Reneau, S., Levine, A., 2003. Comparison of SAR techniques for luminescence dating of sediments derived from volcanic tuff. Quaternary Science Reviews 22, 1131–1138.
Lepper, K., Fisher, T.G., Hajdas, I., Lowell, T.V., 2007. Ages for the Big Stone moraine and the oldest beaches of glacial Lake Agassiz: implications for deglaciation chronology. Geology 35, 667–670.
Lepper, K., Gorz, K.L., Fisher, T.G., Lowell, T.V., 2011. Age determinations for Lake Agassiz shorelines west of Fargo, North Dakota, U.S.A. Canadian Journal of Earth Sciences 48, 1199–1207.
Lowe, J.J., Rasmussen, S.O., Bjorck, S., Hoek, W.Z., Steffensen, J.P., Walker, M.J.C., Yu, Z.C., 2008. Synchronisation of palaeoenvironmental events in the North Atlantic region during the Last Termination: a revised protocol recommended by the INTIMATE group. Quaternary Science Reviews 27, 6–17.
Lowell, T.V., Hayward, R.K., Denton, G.H., 1999. The Role of Climate Oscillations in Determining Ice Margin Position: Hypothesis, Examples, and Implications. In: Mickelson, D.M., Attig, J.W. (Eds.), Glacial Processes: Past and Present. : Geological Society of America Special Paper, 337. Geological Society of America, Boulder, CO, pp. 193–203.

Matsch, C.L., 1983. River Warren, the Southern Outlet to Glacial Lake Agassiz. In: Teller, J.T., Clayton, L. (Eds.), Glacial Lake Agassiz. Geological Association of Canada Special Paper, 26. University of Toronto Press, pp. 231–244.
Murray, A., Wintle, A.G., 2000. Luminescence dating of quartz using and improved single-aliquot regenerative protocol. Radiation Measurements 32, 571–577.
Prescott, J.R., Hutton, J.T., 1988. Cosmic-ray and gamma-ray dosimetry for TL and electron-spin-resonance. Nuclear Tracks and Radiation Measurements 14, 223–227.
Prescott, J.R., Hutton, J.T., 1994. Cosmic ray contributions to dose rates for luminescence and ESR dating: large depths and long-term time variations. Radiation Measurements 23, 497–500.
Rayburn, J.A., 1997. Correlation of the Campbell strandlines along the northwestern margin of Glacial Lake Agassiz. Unpublished M.Sc. thesis. University of Manitoba.
Rayburn, J.A., Teller, J.T., 2007. Isostatic rebound in the northwestern part of the Lake Agassiz basin: Isobase changes and overflow. Palaeogeography, Palaeoclimatology, Palaeoecology 246, 23–30.
Risberg, J., Matile, G., Teller, J.T., 1995. Lake Agassiz water level changes as recorded by sediments and their diatoms in a core from southeastern Manitoba, Canada. PACT 50, 85–96.
Ruhe, R.V., 1969. Quaternary landscapes in Iowa. Iowa State University Press, Ames (253 pp.).
Teller, J.T., Risberg, J., Matile, G., Zoltai, S., 2000. Postglacial history and paleoecology of Wampum, Manitoba, a former lagoon in the Lake Agassiz basin. Geological Society of America Bulletin 112 (6), 943–958.
Upham, W., 1895. The Glacial Lake Agassiz. United States Geological Survey Monograph 25, 685.
Weller, M.B., Fisher, T.G., 2009. Feasibility study of mapping continuous strandlines along the southeast Lake Agassiz basin. Journal of Maps 2009, 152–165.
Wintle, A.G., Murray, A., 2006. A review of quartz optically stimulated luminescence characteristics and their relevance in single-aliquot regeneration dating protocols. Radiation Measurements 41, 369–391.
Yang, Z., Teller, J.T., 2012. Using LiDAR Digital Elevation Model data to map Lake Agassiz beaches, measure their isostatically-induced gradients, and estimate their ages. Quaternary International 260, 32–42.